

Helical Twist controls the thickness of F-actin bundles

M.M.A.E. Claessens, C. Semmrich and A.R. Bausch

E22-Biophysics, Technische Universität München, James Franck Straße, 85747 Garching, Germany

4 June 2007

In the presence of condensing agents such as non-adsorbing polymer, multivalent counter ions and specific bundling proteins chiral biopolymers typically form bundles with a finite thickness rather than phase separating into a polymer rich phase¹⁻⁵. Although short range repulsive interactions or geometrical frustrations are thought to force the equilibrium bundle size to be limited⁶, the precise mechanism is yet to be resolved. The importance of the tight control of biopolymer bundle size is illustrated by the ubiquitous cytoskeletal F-actin filament bundles that are crucial for the proper function of cells⁷. Using an *in vitro* model system we show that size control relies on a mismatch between the helical structure of individual actin filaments and the geometric packing constraints within bundles. Actin binding proteins change the twist of filamentous actin in a concentration dependent manner. The energetic trade-off between filament twisting and cross-linker binding within a bundle is suggested as the fundamental mechanism by which cells can precisely adjust bundle size and strength. The proposed mechanism is generic and has important implications for the size control of other biopolymer aggregates.

Bundles of filamentous actin (F-actin) are key components of the eukaryotic cytoskeleton and are generally used for mechanical support. In filopodia, microvilli and stereocilia F-actin bundles fortify cellular protrusions, while in stress-fibers they help to

maintain cellular integrity. The appearance of parallel F-actin bundles is tightly controlled by a myriad of actin binding proteins (ABPs). Moreover, cytoskeletal processes that involve F-actin bundles typically all employ their own complements of multiple ABPs⁷. Although this is probably at least partly related to the specific mechanical requirements of the different structures^{8,9}, the well defined length, thickness and organization of the various cytoskeletal F-actin bundles might necessitate the use of a combination of different ABPs. Loss of one of the ABPs typically affect either the organization or the thickness of the bundles^{7,10-12}, mutations often result in diseases^{13,14}.

In vitro reconstituted F-actin bundles also form ordered bundles of sizes comparable to those is found *in vivo*. In the presence of non-adsorbing polymer and/or multivalent counterions charged biopolymers such as F-actin, microtubules, or DNA generally form an equilibrium phase of bundles with a well defined thickness^{1-5,15-17}. The stabilization mechanism of these bundles is proposed to be similar to that of equilibrium colloidal clusters^{18,19}; steric and short range electrostatic interactions or frustration within the bundles prevent charge neutralization and limit the equilibrium bundle size⁶. Although there are indications that, *in vitro*, the diameter of ABP/F-actin bundles is well defined, reconstructed ABP/actin bundles are typically embedded in a continuous isotropic background network which has prevented a clear description or quantitative analysis²⁰⁻²². The ABP fascin organizes actin filaments into a cross-linked network of bundles in which no single filaments can be observed²³. This makes reconstituted F-actin/fascin system ideally suited to resolve the mechanism underlying the finite size of F-actin/ABP bundles.

Here we investigate the thickness and organization of actin filaments bundled by fascin and show that the helical structure of F-actin and the packing symmetry within the bundle are essential for the control of bundle thickness. F-actin/fascin bundles display a uniform thickness and are straight over long distances reflecting their high bending rigidity⁸. The bundle thickness is independent of the actin concentration but depends exclusively on the

molar ratio between bound fascin and G-actin R^* . When the actin concentration is increased at constant $R=1$ a decrease of the mesh size rather than an increase in bundle diameter is observed (Fig. 1A, B). The thickness of the F-actin/fascin bundles can be extracted from electron micrographs by fitting a Gaussian to the intensity profiles (Fig. 1C inset). The bundle thickness distributions obtained in this way are very uniform and show a slight increase of the bundle diameter, D with the fascin concentration $D \sim (R^*)^{0.2}$ (Fig. 1C). Increasing amounts of fascin are needed to add the next filament to the bundle, as the number of filaments in a bundle scales as $n_f \sim D^2$. Interestingly, D reaches a plateau at $R^* \approx 0.3-0.4$; a further increase of the fascin concentration has no influence on the bundle diameter. The observed thickness of F-actin/fascin bundles is independent of the preparation procedure. Whether long or shortened pre-polymerized filaments are incubated with fascin, or fascin is already present during the polymerization process does not affect D .

It is not a priori clear why bundles with such a well defined diameter are observed, or what causes the bundle thickness to be limited. The bundle diameter could in principle be either kinetically²⁴ or thermodynamically⁶ constrained. However, the independence of the bundle diameter on the preparation method and system used, strongly suggests an equilibrium mechanism. While charge accumulation has been suggested to prevent clusters of charged colloidal particles to grow beyond a certain size²⁵, this is not the case for ABP/F-actin bundles. The separation between F-actin filaments bundled with fascin is approximately 5 nm, much larger than the Debye length at the ionic strength used. Decreasing the salt concentration to the minimum necessary for actin polymerization (2mM MgCl₂, no KCl or CaCl₂) has therefore no influence on the maximum F-actin/fascin bundle thickness. As electrostatic repulsion between actin filaments is too short ranged to affect bundle assembly other mechanisms have to be responsible for preventing bundles from growing thicker.

To precisely quantify the finite and limited thickness of actin bundles a mesoscopic system is advantageous. The recently introduced emulsion droplet system seems extremely

well suited for this purpose²⁶. At small droplet diameters, D_d , F-actin filaments bundle into a single ring in the presence of fascin⁸. With increasing droplet diameter this ring splits into two. In the largest droplets complicated structures are found (Fig. 2A-C). The total mass of F-actin within a drop, or equivalently, its total length L , can be computed very precisely from the actin concentration and droplet diameter. Moreover, the bundle radius can be measured and for the case of a single ring the number of filaments n_f in the bundle can be deduced. We observe that a confined single bundle does not become thicker than ~ 20 filaments (Fig. 2E). Instead of growing thicker rings, filaments rather organize into more bundles upon increasing droplet diameter or actin concentration.

TEM micrographs of adsorbed actin rings extracted from emulsion droplets show closely packed F-actin/fascin bundles with a typical diameter of 5-6 filaments (Fig. 2D). Considering the expected hexagonal packing²⁷, this is in excellent agreement with the ~ 20 filaments per bundle estimated from figure 2E. A geometrical argument shows that for bundles with $n_f < 20$ not all possible cross-linker binding sites are occupied, while the maximum size observed experimentally agrees with full occupation of all possible binding sites (Supplementary Material). Growth of the bundles is not prevented by a lack of ABP but instead seems to be physically limited to 2 hexagonal shells of actin filaments.

To investigate the microscopic bundle geometry more closely, we performed SAXS experiments. Figure 3A shows a typical 2D diffraction pattern of partially aligned F-actin/fascin bundles, Fig. 3B depicts circularly averaged intensities for different R values. The appearance of the sharp q_{10} peak at 0.585 nm^{-1} for $R^* > 0.1$ is indicative of bundle formation (Fig. 3B). The individual actin filaments in these bundles are packed onto a hexagonal lattice with a centre to centre distance of $4\pi/\sqrt{3}(q_{10})=12.4 \text{ nm}$. Besides the q_{10} , $q_{01}=\sqrt{3}q_{10}$, $q_{20}=2q_{10}$ and $q_{21}=\sqrt{7}q_{10}$ peaks characteristic of hexagonal packing, the convolution of the hexagonal bundle structure and the helical F-actin structure results in additional peaks that appear along q_z (Fig. 3C). In the absence of fascin the actin filament displays a $-13/6$ symmetry

characterized by diffraction peaks at 1.14 and 1.25 nm⁻¹. These peaks correspond to the 6th and 7th layer lines (n=1 and n=-1 Bessel functions) which are much more intense than the other layer lines and dominate the diffraction pattern of partially aligned F-actin. The position of these peaks gradually shifts with increasing fascin concentration until at R=0.3-0.4 the convolution of the helical F-actin structure and the hexagonal bundle structure results in peaks at 1.20, 1.35 and 1.46 nm⁻¹ (Fig. 3C). The corresponding maximum overtwist of ~0.9° per actin monomer agrees with the overtwist observed for F-actin/espil bundles²⁸.

The energetic cost involved in overtwisting F-actin will have to be provided for by fascin binding. The twist energy can be obtained for each value of R from the torsional stiffness τ ($\tau=2/3\kappa=4.6 \cdot 10^{-26}$ Nm² where κ is the bending stiffness), actin monomer spacing (2.7 nm), and the observed overtwist. The overtwist is computed assuming a linear relation between the position of the 6th layer line and the overtwist. The twist energy per actin monomer increases with the number of filaments in the bundle (Fig 4). For all fascin and actin concentrations the gain in binding energy per actin monomer is always slightly larger than the loss in torsional energy per actin monomer (Fig 4). The energy necessary for twisting turns out to be approximately 10k_BT per bound fascin, while fascin binding provides $\Delta G = k_B T \ln(K_D) \sim 15$ k_BT per bound fascin molecule.

The original -13/6 helical symmetry of individual actin filaments is apparently not ideally suited for hexagonal packing^{2,27}. To fit the filaments on a hexagonal lattice ABPs have to twist or locally stretch the F-actin. The -28/13 symmetry observed for the saturated F-actin/fascin bundles is still suboptimal for hexagonal packing and bundle thickness is therefore limited. Growing thicker bundle would require more filament torsion and hence more fascin. The number of fascin binding sites along an actin filament is however limited which prevents the bundles from growing beyond ~20 filaments.

It thus seems that nature deliberately chose to have a mismatch between the pitch of individual helical polymers and the optimum value required for hexagonal packing in order to

implement an intrinsic limit to bundle growth. Moreover, the helical structure of actin filaments is affected by several ABPs²⁷⁻³⁰ suggesting that this conformational variability of F-actin is exploited in many cytoskeletal processes. By adapting the twist, tilt, and rotation of actin filaments in the acrosomal bundle, the ABP scriuin is thought to store energy in the actin helix that can subsequently be used in the acrosomal process^{29,31}. Similarly, the variable twist of the actin filament may be utilized by nature to regulate the often well defined thickness observed for F-actin bundles found in microvilli, filopodia and stereocilia. The control of bundle thickness by the helical twist and packing constraints gives an alternative explanation for the use of multiple ABPs in one bundle. Since fascin gives rise to well organized but rather thin bundles additional ABPs might be required to link these bundles in larger structures as was observed in *Drosophila* bristles¹⁰.

In conclusion we have shown that the geometric constraints imposed by the helical structure of actin filaments are exploited to tightly control bundle thickness. The balance between mechanical twisting energy costs and gains in binding energy regulates actin bundle formation and growth. Instead of twisting the filaments in the bundle, mechanical strain involved in bundling chiral polymers can in principle also result in a supertwist of the bundles affecting the resulting functional structures^{32,33}. The supercoiling observed for filamin/actin bundle rings in vesicles might be a first indication that there are indeed some ABPs that supertwist the whole bundle rather than overtwist the individual filaments³⁴. By using chiral biopolymers, cells create the opportunity to exploit a sensitive balance of mechanical and biochemical means to control the thickness of F-actin bundles.

Methods

Lyophilized G-actin from rabbit skeletal muscle³⁵ was dissolved in deionized water, dialyzed against G-buffer (2mM Tris, 0.2mM ATP, 0.2mM CaCl₂, 0.2mM DTT and 0.005% NaN₃, pH 8), stored at 4°C and used within seven days after preparation. Recombinant human fascin was expressed in *Escherichia coli* BL21-codon+ bacteria as described before^{8,36}. F-

actin/fascin networks were constructed by polymerizing G-actin in the presence of fascin in F-buffer (2mM Tris, 0.5mM ATP, 0.2mM CaCl₂, 2mM MgCl₂, 100mM KCl, 0.2mM DTT, pH 7.5) at 20 °C. To visualize the network, F-actin filaments were fluorescently labeled using TRITC-phalloidin. Emulsion droplets containing F-actin/fascin bundles were prepared as described before^{8,26}. Samples for transmission electron microscopy (Philips EM400T) were adsorbed to glow-discharged carbon-coated formvar films on copper grids and negatively stained with 0.8% uranyl acetate, excess liquid was drained with filter paper. To be able to compare experiments performed at different actin concentrations the molar ratio, R , between fascin and actin, $R = c_f/c_a$ was translated into an effective R^* , assuming an equilibrium dissociation constant $K_d=0.5\mu\text{M}$ and $R^*=R(c_{ABP}/(K_d+c_{ABP}))$.

Synchrotron small angle x-ray experiments have been performed on the ID-2 beamline at the ESRF Grenoble, France. For these experiments F-actin/fascin networks were polymerized in 1.5 mm quartz capillaries at actin concentrations between 0.8 and 5 mg/ml. These samples showed powder scattering, to be able to discern correlations between different directions the actin bundles were partially aligned using a flow cell. The scattering was done at 12.46 keV and a sample to-detector distance of 1m. Scans were performed for 0.5-6 seconds, over this time no radiation damage was observed. The diffraction data were analyzed using EDF-plot³⁷.

Acknowledgements

The authors would like to thank M. Rusp for the actin preparation, L. Ramos and E. Di Cola for their help with the SAXS experiments, and K. Kroy, R. Netz and H. Wada for interesting and useful discussions. This work was supported by Deutsche Forschungsgemeinschaft through the DFG-Cluster of Excellence Munich-Centre for Advanced Photonics and SFB413.

References

1. Hosek, M. & Tang, J. X. Polymer-induced bundling of F actin and the depletion force. *Phys. Rev. E* **69**, 051907 (2004).
2. Angelini, T. E., Liang, H., Wriggers, W. & Wong, G. C. L. Like-charge attraction between polyelectrolytes induced by counterion charge density waves. *Proc. Natl. Acad. Sci. USA* **100**, 8634-8637 (2003).
3. Needleman, D. J. et al. Higher-order assembly of microtubules by counterions: From hexagonal bundles to living necklaces. *Proc. Natl. Acad. Sci. USA* **101**, 16099-16103 (2004).
4. Conwell, C. C., Vilfan, I. D. & Hud, N. V. Controlling the size of nanoscale toroidal DNA condensates with static curvature and ionic strength. *Proc. Natl. Acad. Sci. USA* **100**, 9296-9301 (2003).
5. Bloomfield, V. A. DNA condensation by multivalent cations. *Biopolymers* **44**, 269-282 (1997).
6. Henle, M. L. & Pincus, P. A. Equilibrium bundle size of rodlike polyelectrolytes with counterion-induced attractive interactions. *Phys. Rev. E* **71** (2005).
7. Bartles, J. R. Parallel actin bundles and their multiple actin-bundling proteins. *Curr. Opin. Cell Biol.* **12**, 72-78 (2000).
8. Claessens, M. M. A. E., Bathe, M., Frey, E. & Bausch, A. R. Actin-binding proteins sensitively mediate F-actin bundle stiffness. *Nature Mat.* **5**, 748-753 (2006).
9. Bathe, M., Heussinger, C., Claessens, M. M. A. E., Bausch, A. R. & Frey, E. Mechanics of nanofiber bundles. *submitted* (2006).
10. Tilney, L. G., Connelly, P. S., Vranich, K. A., Shaw, M. K. & Guild, G. M. Why are two different cross-linkers necessary for actin bundle formation in vivo and what does each cross-link contribute? *J. Cell Biol.* **143**, 121-133 (1998).
11. Tilney, L. G., Connelly, P. S., Vranich, K. A., Shaw, M. K. & Guild, G. M. Regulation of actin filament cross-linking and bundle shape in *Drosophila* bristles. *J. Cell Biol.* **148**, 87-99 (2000).
12. Guild, G. M., Connelly, P. S., Ruggiero, L., Vranich, K. A. & Tilney, L. G. Actin filament bundles in *Drosophila* wing hairs: Hairs and bristles use different strategies for assembly. *Mol. Biol. Cell* **16**, 3620-3631 (2005).
13. Cant, K., Knowles, B. A., Mooseker, M. S. & Cooley, L. *Drosophila* Singed, a Fascin Homolog, Is Required for Actin Bundle Formation During Oogenesis and Bristle Extension. *J. Cell Biol.* **125**, 369-380 (1994).
14. Zheng, L. L. et al. The deaf jerker mouse has a mutation in the gene encoding the espin actin-bundling proteins of hair cell stereocilia and lacks espins. *Cell* **102**, 377-385 (2000).
15. Tharmann, R., Claessens, M. M. A. E. & Bausch, A. R. Micro- and macrorheological properties of actin networks effectively crosslinked by depletion forces. *Biophys. J.* **90**, 2622-2627 (2006).
16. Tang, J. X. & Janmey, P. A. The polyelectrolyte nature of F-actin and the mechanism of actin bundle formation. *J. Biol. Chem.* **271**, 8556-8563 (1996).
17. Strey, H. H., Podgornik, R., Rau, D. C. & V.A., P. DNA-DNA interactions. *Current Opinion in Structural Biology* **8**, 309-313 (1998).
18. Segre, P. N., Prasad, V., Schofield, A. B. & Weitz, D. A. Glasslike kinetic arrest at the colloidal-gelation transition. *Phys. Rev. Lett.* **86**, 6042-6045 (2001).
19. Stradner, A. et al. Equilibrium cluster formation in concentrated protein solutions and colloids. *Nature* **432**, 492-495 (2004).

20. Tempel, M., Isenberg, G. & Sackmann, E. Temperature-induced sol-gel transition and microgel formation in alpha-actinin cross-linked actin networks: A rheological study. *Phys. Rev. E* **54**, 1802-1810 (1996).
21. Wagner, B., Tharmann, R., Haase, I., Fischer, M. & Bausch, A. R. Cytoskeletal polymer networks: The molecular structure of cross-linkers determines macroscopic properties. *Proc. Natl. Acad. Sci. USA* **103**, 13974-13978 (2006).
22. Bausch, A. R. & Kroy, K. A bottom-up approach to cell mechanics. *Nature Phys.* **2**, 231-238 (2006).
23. Lieleg, O., Claessens, M. M. A. E., Heussinger, C., Frey, E. & Bausch, A. R. Mechanics of bundled semiflexible polymer networks. *submitted* (2006).
24. Kierfeld, J., Kuhne, T. & Lipowsky, R. Discontinuous unbinding transitions of filament bundles. *Phys. Rev. Lett.* **95** (2005).
25. Groenewold, J. & Kegel, W. K. Anomalously large equilibrium clusters of colloids. *J. Phys. Chem. B* **105**, 11702-11709 (2001).
26. Claessens, M. M. A. E., Tharmann, R., Kroy, K. & Bausch, A. R. Microstructure and viscoelasticity of confined semiflexible polymer networks. *Nature Phys.* **2**, 186-189 (2006).
27. DeRosier, D. J. & Tilney, L. G. How Actin-Filaments Pack into Bundles. *Cold Spring Harbor Symposia on Quantitative Biology* **46**, 525-540 (1981).
28. Purdy, K. R., Bartles, J. R. & Wong, G. C. L. Structural polymorphism of the actin-espino system: a prototypical system of filaments and linkers in stereocilia. *Phys. Rev. Lett.* **98**, 058105 (2007).
29. Derosier, D., Tilney, L. & Flicker, P. Change in the Twist of the Actin-Containing-Filaments Occurs During the Extension of the Acrosomal Process in Limulus Sperm. *J. Mol. Biol.* **137**, 375-389 (1980).
30. Stokes, D. L. & DeRosier, D. J. The Variable Twist of Actin and Its Modulation by Actin-Binding Proteins. *J. Cell Biol.* **104**, 1005-1017 (1987).
31. Schmid, M. F., Sherman, M. B., Matsudaira, P. & Chiu, W. Structure of the acrosomal bundle. *Nature* **431**, 104-107 (2004).
32. Grason, G. M. & Bruinsma, R. F. Chirality and Equilibrium Biopolymer Bundles. *cond-mat arXiv:0705.0392v1* (2007).
33. Kamien, R. D. & Nelson, D. R. Iterated Moire Maps and Braiding of Chiral Polymer Crystals. *Phys. Rev. Lett.* **74**, 2499-2502 (1995).
34. Limozin, L. & Sackmann, E. Polymorphism of cross-linked actin networks in giant vesicles. *Physical Review Letters* **89**, 168103 (2002).
35. Spudich, J. A. & Watt, S. Regulation of Rabbit Skeletal Muscle Contraction .1. Biochemical Studies of Interaction of Tropomyosin-Troponin Complex with Actin and Proteolytic Fragments of Myosin. *J. Biol. Chem.* **246**, 4866-71 (1971).
36. Ono, S. et al. Identification of an actin binding region and a protein kinase C phosphorylation site on human fascin. *J. Biol. Chem.* **272**, 2527-2533 (1997).
37. Sztucki, N. & Narayanan, T. Development of an ultra-small-angle X-ray scattering instrument for probing the microstructure and the dynamics of soft matter. *J. Appl. Cryst.* **40**, s459-s462 (2007).

Figures

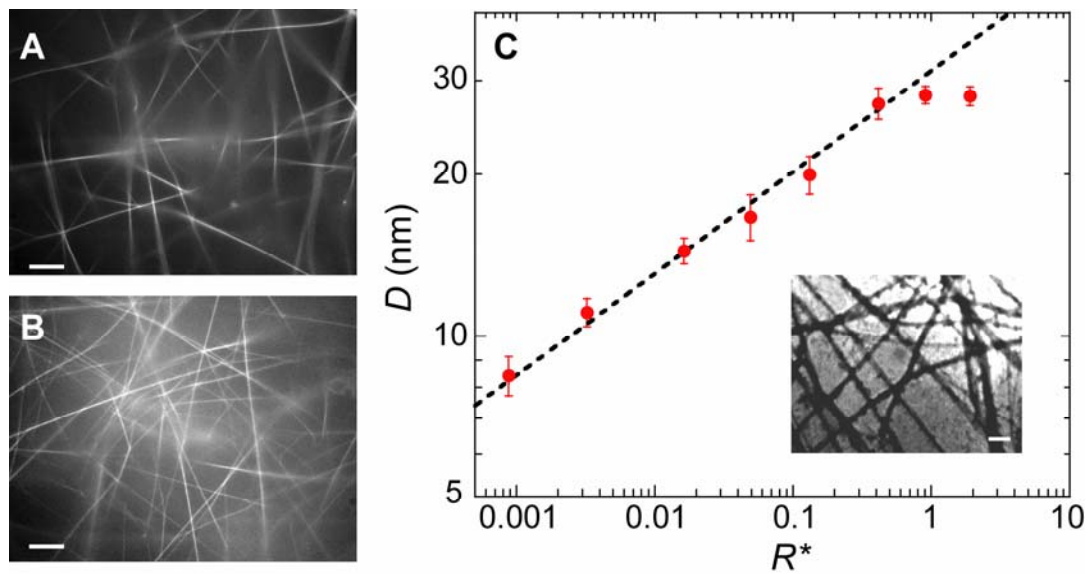


Fig. 1 (A, B) Fluorescence micrographs of TRITC phalloidin labeled actin bundles. The bundles are cross-linked with fascin ($R = 1$). Increasing the actin concentration from 0.04 mg/ml (A) to 0.1 mg/ml (B) merely increases the mesh size and seems to have no effect on the bundle thickness. The scale bar indicates 10 μm . **(C)** Bundle diameters D obtained from TEM micrographs (inset) as a function of R .

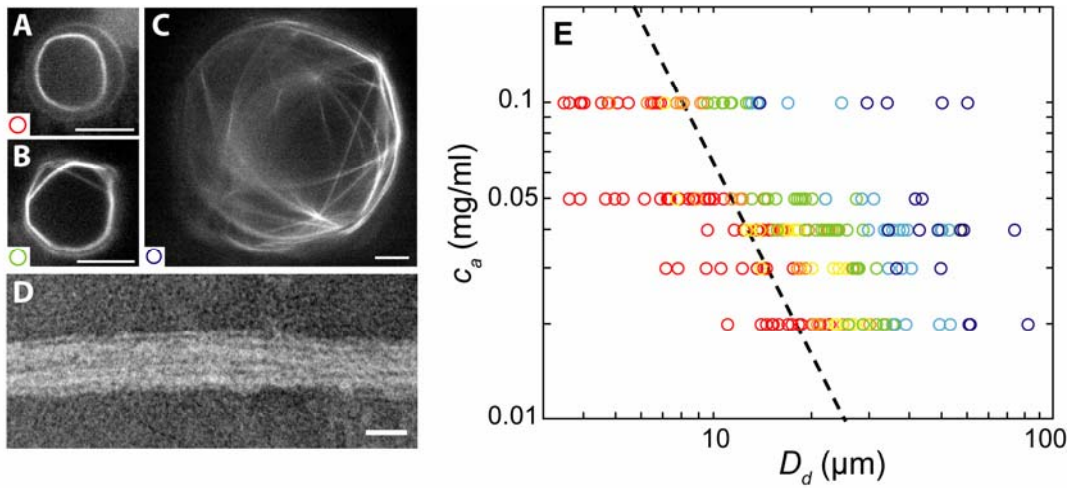


Fig. 2 (A-C) Fluorescent micrographs of TRITC phalloidin labeled F-actin/fascin bundles ($R=1$). For small droplet diameters filaments organize into a single ring (\circ), in larger droplets a second bundle appears (\circ), more complicated structures are found in very large droplets (\circ). The scale bar indicates $10\ \mu\text{m}$ (**D**) TEM micrograph of a detail of an actin bundle obtained from the confined rings showing the typical bundle diameter of approximately 5 filaments (scale bar $20\ \text{nm}$). (**E**) The organization of actin bundles as a function of the actin concentration c_a and emulsion droplet diameter D_d . The colors depicted in the diagram represent the different structures presented in (A-C). A single bundle does not grow thicker than ~ 20 filaments, the dotted line represents $n_f=20$.

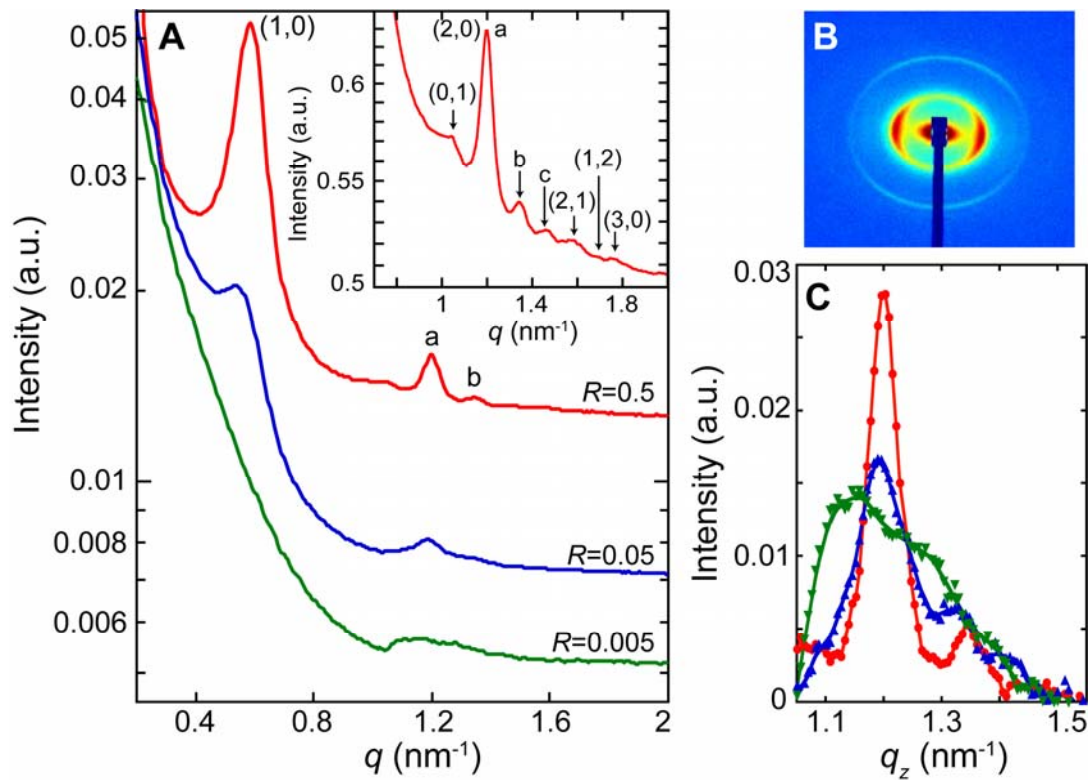


Fig. 3 (A) Circularly averaged diffraction data for different R values and $c_a=2$ mg/ml. For $R \geq 0.01$ peaks related to hexagonal packing of filaments appear. A magnification of the diffraction at $R=0.5$ is shown in the inset. The peaks belonging to the layer lines are indexed a, b and c. **(B)** A typical 2D diffraction pattern of a partially aligned F-actin/fascin network obtained by SAXS experiments for $R=0.5$ and $c_A=2$ mg/ml. **(C)** Angularly averaged wedges along the axial direction q_z . Peaks corresponding to the helical structure of the actin filaments shift with R . ($R=0.005$ \blacktriangledown , $R=0.05$ \blacktriangle , $R=0.5$ \bullet)

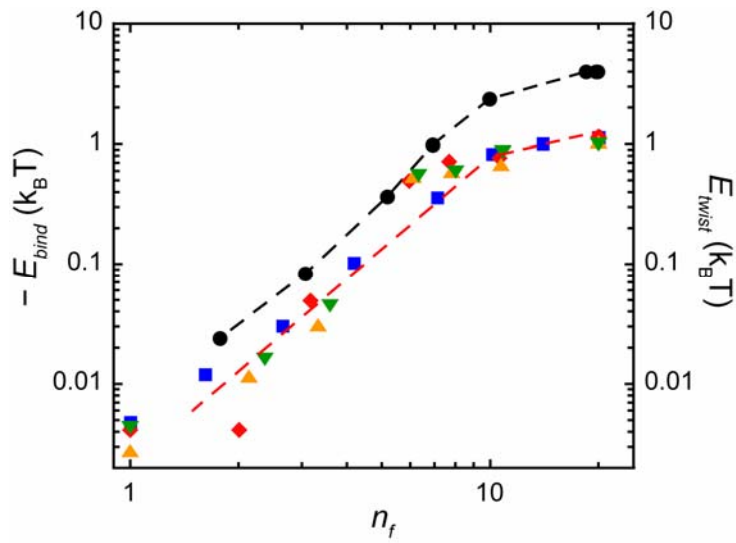


Fig. 4 (C) The energy costs for filament twisting (●) and gain in binding energy ($c_a=0.8$ mg/ml ■, 1.6 mg/ml ◆, 2 mg/ml ▲, 3 mg/ml ▼) as a function of the number of filaments in the bundle n_f . The energies are given per actin monomer.

Online Material

Methods

G-actin was prepared from rabbit skeletal muscle and stored in lyophilized form at -20°C ¹. The lyophilized actin was dissolved in deionized water and dialyzed against G-buffer (2mM Tris, 0.2 mM ATP, 0.2 mM CaCl_2 , 0.2 mM DTT and 0.005% NaN_3 , pH 8) at 4°C . G-actin solutions were stored at 4°C and used within seven days after preparation. Recombinant human fascin was expressed in *Escherichia coli* BL21-codon+ bacteria as described before^{2,3}. In the experiments the molar ratio, R , between fascin and actin, $R = c_f/c_a$ was varied between 0.01 and 2. To be able to compare experiments performed at different actin concentrations R was translated into an effective R , R^* , assuming an equilibrium dissociation constant $K_d = 0.5 \mu\text{M}$ and $R^* = R \cdot (c_{\text{ABP}} / (K_d + c_{\text{ABP}}))$.

The F-actin/fascin networks were constructed by polymerizing G-actin in the presence of fascin in F-buffer (2mM Tris, 0.5 mM ATP, 0.2 mM CaCl_2 , 2 mM MgCl_2 , 100mM KCl, 0.2 mM DTT, pH 7.5) at 20°C . To visualize the network, F-actin filaments are fluorescently labeled using TRITC-phalloidin. Emulsion droplets containing F-actin/fascin bundles were prepared as described before⁴. Samples for transmission electron microscopy (Philips EM 400T) were adsorbed to glow-discharged carbon-coated formvar films on copper grids. The grids are washed in a drop of distilled water and negatively stained with 0.8% uranyl acetate, excess liquid was drained with filter paper.

Synchrotron small angle x-ray experiments have been performed on the ID-2 beamline at the ESRF Grenoble, France. For these experiments F-actin/fascin networks were polymerized in 1.5 mm quartz capillaries at actin concentrations between 0.8 and 5 mg/ml. These samples showed powder scattering and images were therefore averaged over 360° . To be able to discern correlations between different directions the actin bundles were partially aligned using a flow cell. The scattering was done at 12.46 keV and a sample to-detector distance of 1 m. Scans were performed for 0.5-6 seconds, over this time no radiation damage was observed. The diffraction data were analysed using EDF-plot⁵.

Bundle Geometry

A geometrical argument demonstrates why the bundles do not grow thicker than 20 filaments. In a system with a given total amount of actin only a limited number of bundles consisting of n_f filaments can be obtained. The amount of fascin that can bind to a filament is limited, an actin filament with 6 fascin binding sites consists of approximately 13 actin monomers. Assuming that all bundles have the same thickness and all binding sites are occupied, the

number of filaments in one bundle, n_f is determined by the ratio between the total number of cross-linker n_{cl}^t and actin monomers n_a^t in the system $n_{cl}^t / n_a^t = R = 1/13(3 + 3.5n_f^{-1/2})$. For building less but thicker bundles that are fully saturated with cross-linking molecules, decreasing amounts of cross-linkers are needed. To compare the R values at which fully saturated bundles of n_f filaments are obtained with the experimentally observed values, the $D(R_{eff})$ curve (Fig. 1C) has to be translated into a $R(n_f)$. To obtain $R(n_f)$ it is assumed that $D \sim n_f^{1/2}$ and that the maximum bundle thickness observed in bulk networks is ~ 20 filaments as observed in confinement (Fig. 2E). Interestingly, for bundles with $n_f < 20$ not all possible cross-linker binding sites are occupied, while the maximum size observed experimentally agrees with full occupation of all possible binding sites.

1. Spudich, J. A. & Watt, S. Regulation of Rabbit Skeletal Muscle Contraction .1. Biochemical Studies of Interaction of Tropomyosin-Troponin Complex with Actin and Proteolytic Fragments of Myosin. *J. Biol. Chem.* **246**, 4866-71 (1971).
2. Ono, S. et al. Identification of an actin binding region and a protein kinase C phosphorylation site on human fascin. *J. Biol. Chem.* **272**, 2527-2533 (1997).
3. Claessens, M. M. A. E., Bathe, M., Frey, E. & Bausch, A. R. Actin-binding proteins sensitively mediate F-actin bundle stiffness. *Nature Mat.* **5**, 748-753 (2006).
4. Claessens, M. M. A. E., Tharmann, R., Kroy, K. & Bausch, A. R. Microstructure and viscoelasticity of confined semiflexible polymer networks. *Nature Phys.* **2**, 186-189 (2006).
5. Sztucki, N. & Narayanan, T. Development of an ultra-small-angle X-ray scattering instrument for probing the microstructure and the dynamics of soft matter. *J. Appl. Cryst.* **40**, s459-s462 (2007).